This is the published version of a paper published in *Physical Review A. Atomic, Molecular, and Optical Physics.*

Permanent link to this version:
http://urn.kb.se/resolve?urn=urn:nbn:se:du-11216

Adiabatic propagation in potential structures

Markku Jääskeläinen and Stig Stenholm

Laser Physics and Quantum Optics, Royal Institute of Technology, Roslagstullsbacken 21 SE-10691 Stockholm, Sweden
(Received 3 December 2001; published 26 August 2002)

In this work the adiabatic approximation is applied to the propagation of matter waves in confined geometries like those experimentally realized in recent atom optical experiments. Adiabatic propagation along a channel is assumed not to mix the various transverse modes. Nonadiabatic corrections arise from the potential squeezing and bending. Here we investigate the effect of the former. Detailed calculations of two-dimensional propagation are carried out both exactly and in an adiabatic approximation. This offers the possibility to analyze the validity of adiabaticity criteria. A semiclassical (sc) approach, based on the sc Massey parameter is shown to be inadequate, and the diffraction due to wave effects must be included separately. This brings in the Fresnel parameter well known from optical systems. Using these two parameters, we have an adequate understanding of adiabaticity on the system analyzed. Thus quantum adiabaticity must also take cognizance of the intrinsic diffraction of matter waves.

I. INTRODUCTION

The recent experimental progress in time-dependent quantum dynamics has created an interest in localized quantum states propagating through various types of potential structures. In communication technology, the progress of an optical pulse through guiding structures serves as the model system for both communication and computation applications. In femtosecond laser-induced dynamics of molecular processes, we have a well established area of research, where vibrational states propagate along electronic potential surfaces. The advances in cooling and trapping [1] of neutral atoms have led to the possibility to confine atomic wave functions to low-dimensional structures, thus creating the analog of electronic nanostructures but for neutral atoms. Several techniques have been utilized [2], among them magnetic confinement both inside hollow glass tubes [3] and above current carrying wires [4], light force trapping in hollow fibers [5], and various other schemes based on the interaction of electromagnetic radiation with atoms. In confinement to atomic waveguide geometries with transverse dimensions around or below micrometer scales, the quantum nature of the atoms starts to influence the dynamics. Propagation in such potentials will take place in the form of matter waves, we are in the regime of atom optics, and the phenomena can be used to explore new features involving the fundamental properties of quantum dynamics.

In waveguides for photons or their atomic counterparts, we assume that the wave packet describing the propagation follows the channel smoothly and without too much distortion. The use of single-mode fibers is based on this assumption. Molecular vibrational states are supposed to progress on the Born-Oppenheimer surfaces without being too perturbed by nonadiabatic influences. Such assumptions derive from some underlying smoothness of the guiding structures; when this is not the case, the adiabaticity ceases to hold and new phenomena can be expected. It is the purpose of our investigations to consider such effects and attempt to find the parameter regions where they may be neglected. The present paper reports our first results in this direction.

The adiabatic theorem was formulated in the old quantum theory by Ehrenfest [6] and it formed the basis for later works. Born and Fock [7,8] emphasized the importance of adiabatic invariants in quantum mechanics. As a mathematical tool, adiabatic methods have been used in many different contexts [9], and they have usually turned out to be highly successful; in fact, often beyond what could be expected from naïve validity arguments. We here ask the question, when a wave packet propagating according to Schrödinger's equation can be described by an adiabatic ansatz. This question has become exceedingly interesting in the effort to extend optical and electronic nanostructure devices to atomic states, for instance quantum point contacts [10] and directional couplers [11].

Wave-packet dynamics has proved to be a very useful tool for studies of dynamics in quantum systems, to device simple models and interpret experiments [12]. To simulate realistic systems, one needs to consider many degrees of freedom, which makes the numerical work difficult and in many cases well beyond the resources of even the most powerful modern computers. Due to the exponential growth of Hilbert space with the number of degrees of freedom, well known in quantum information theory, the amount of data to be processed increases exponentially with the number of dimensions. Any method that reduces this number is extremely interesting and will find uses in diverse areas. The use of separated channels or modes offers such an approach, but this requires certain adiabaticity assumptions to hold.

In molecular dynamics, Marcus [13], Wu and Levine [14] pioneered the use of separated variables in local coordinate systems along the reaction path. These may then be used for propagation of wave packets on the reaction surfaces. It has also been suggested that population inversion could be induced by the curvature of the minimal path which couples the states [15]. These techniques have become widely used in the theory of chemical reactions [16,17] as a method to reduce the numerical complexity of large physical problems.

In this work, propagation of wave packets on two-dimensional potential-energy surfaces is considered. The propagating state is assumed to be localized closely along the

minimal path. An adiabatic basis of discrete eigenstates is used to reduce the complexity of the problem by reducing the time-dependent Schrödinger equation to a set of equations for closely coupled channels. When the physical parameters of the problem allow adiabatic propagation, the discrete basis states decouple making it possible to model the system as a number of independent one-dimensional wave packets propagating in their respective potential structures. As such the model could apply also to chemical reaction pathways, optical communication [18], and mesoscopic structures [19], but we essentially have in mind the recently developed microstructures for confined atomic wave packets.

In the lowest approximation, the center of the wave packet may be assumed to progress along the classical minimum of the potential valley. The transverse curvature is taken to provide a confining potential around this. The first adiabaticity criterion we attempt is a condition stating that the time scale of this potential is shorter than that characterizing the rate of change of the potential. This leads to a criterion for a parameter combination known from semiclassical physics as the Massey parameter. We test this for a signature of adiabaticity, but our numerical work shows that it does not provide enough resolution for this purpose; large ranges of compliance with adiabaticity are possible for each value of this parameter.

In order to progress, a more detailed analysis is required: we find that we need two dimensionless variables to pin down the region where our model system behaves adiabatically. One gives the rate of change of the potential structure and the other one captures the diffractive spreading of the quantum state as compared with the rate of change of the potential structure. Thus we need both parameters to describe the propagation of wave packets in the model. As this only involves squeezing of the channel, but no bending, it is only a partial result; we hope to report on more general investigations in forthcoming publications.

The structure of the paper is as follows: Section II sets up the mathematical structure to be investigated. Section III gives our first attempt at an adiabaticity condition, which is tested in Sec. IV. Analyzing the results in Sec. V, we discover the need for two dimensionless parameters, and we show that these give an adequate description of the adiabatic conditions. Section VI summarizes and concludes the paper.

II. MATHEMATICAL FRAMEWORK

For a general quantum-mechanical problem with time-independent Hamiltonian in a two-dimensional (2D) configuration space the dynamics evolves according to the time-dependent Schrödinger equation

$$i\hbar \frac{\partial \Psi(x,y,t)}{\partial t} = -\frac{\hbar^2}{2m}\nabla^2\Psi(x,y,t) + V(x,y)\Psi(x,y,t).$$

$$(1)$$

In many cases of interest, the propagation will occur along the minimal valleys of the potential-energy surface. Assuming that these minima constitute a smooth, connected curve it

becomes possible to make a coordinate change to a Frenet frame [17] with the path length s along the valley and the distance ξ transverse to the minimal path as coordinates. These coordinates locally define a unique orthonormal coordinate system at each point of the curve. Changing coordinates from (x,y) to (s,ξ), the Laplacian operator transforms into

$$\nabla^2 = \frac{1}{[1+\kappa(s)\xi]}\frac{\partial}{\partial s}\left(\frac{1}{[1+\kappa(s)\xi]}\frac{\partial}{\partial s}\right)$$

$$+ \frac{1}{[1+\kappa(s)\xi]}\frac{\partial}{\partial \xi}\left([1+\kappa(s)\xi]\frac{\partial}{\partial \xi}\right), \quad (2)$$

where $\kappa(s)$ is the curvature of the minimal path. Under the assumption that the minimal curve will bend sufficiently slowly, the Laplacian can be approximated by

$$\nabla^2 \approx \frac{\partial^2}{\partial s^2} + \frac{\partial^2}{\partial \xi^2} - \frac{\partial \kappa(s)}{\partial s}\xi\frac{\partial}{\partial s} + 3\kappa(s)\frac{\partial \kappa(s)}{\partial s}\xi^2\frac{\partial}{\partial s}$$

$$- 2\kappa(s)\xi\frac{\partial^2}{\partial s^2} + \kappa(s)\frac{\partial}{\partial \xi}. \quad (3)$$

Thus curvature gives extra terms that are linear in the derivatives of $\Psi(s,\xi,t)$ with respect to the longitudinal and transverse coordinates. When these are neglected, we obtain an equation equivalent to a two-dimensional Schrödinger equation in Cartesian coordinates

$$i\hbar\frac{\partial \Psi(s,\xi,t)}{\partial t} = -\frac{\hbar^2}{2m}\left(\frac{\partial^2}{\partial s^2} + \frac{\partial^2}{\partial \xi^2}\right)\Psi(s,\xi,t)$$

$$+ V(s,\xi)\Psi(s,\xi,t) + f\left(s,\xi,\frac{\partial \Psi}{\partial s},\frac{\partial^2\Psi}{\partial s^2},\frac{\partial \Psi}{\partial \xi}\right).$$

$$(4)$$

We now assume that the time-independent Schrödinger equation may be solved in the transverse direction at each point along the minimal curve and make an ansatz using the stationary transverse eigenfunctions $\{\eta_n(s,\xi)\}$ as a basis set together with a set of yet unknown longitudinal wave functions, $\{\phi_n(s,t)\}$. These are taken to depend also on time and thus be responsible for propagation in the longitudinal direction. This gives the expansion

$$\Psi(s,\xi,t) = \sum_{n=0}^{\infty}\phi_n(s,t)\eta_n(s,\xi). \quad (5)$$

The set of transverse eigenfunctions satisfies a one-dimensional time-independent Schrödinger equation in the transverse coordinate

$$E_n(s)\eta_n(s,\xi) = -\frac{\hbar^2}{2m}\frac{\partial^2\eta_n(s,\xi)}{\partial \xi^2} + U(s,\xi)\eta_n(s,\xi), \quad (6)$$

and the potential is defined with respect to the local minima of the potential along the transverse direction

$$U(s,\xi) = V(s,\xi) - V(s,0). \tag{7}$$

In many situations, where the main interest lies in exploration of the phenomenology of model systems, detailed knowledge of the potential surface is unnecessary and simplified treatments will capture the interesting effects. Having an analytically solvable potential in the transverse direction greatly simplifies the treatment as this makes it possible to evaluate several quantities of interest. In addition to energies and eigenfunctions also matrix elements for transitions can be obtained as closed analytic expressions. The basic features of any potential having a minimum is reasonably well captured by a harmonic-oscillator potential, given that its anharmonicities are weak. This is often the case in, e.g., molecular and chemical physics. Taylor expanding the potential-energy surface along the transverse coordinate to second order we obtain a parabolic potential

$$V(s,\xi) = V(s,0) + \frac{1}{2} m \omega(s)^2 \xi^2, \tag{8}$$

where the transverse oscillator frequency is given by the curvature with respect to the transverse coordinate

$$\omega(s) = \sqrt{\frac{1}{m} \frac{\partial^2 V(s,0)}{\partial \xi^2}}. \tag{9}$$

The approximation (8) makes it possible to use the harmonic-oscillator eigenfunctions as basis

$$\eta_n(s,\xi) = \left(\frac{1}{\Delta\xi(s)\sqrt{\pi} 2^n n!} \right)^{1/2} e^{-\xi^2/2\Delta\xi(s)^2} H_n\left(\frac{\xi}{\Delta\xi(s)} \right), \tag{10}$$

where the transverse oscillator width is given by

$$\Delta\xi(s) = \sqrt{\frac{\hbar}{m\omega(s)}}; \tag{11}$$

thus determined by the transverse curvature of the potential-energy surface at its bottom. We insert Eqs. (5)–(7) into Eq. (4), multiply by $\eta_m(s,\xi)$ and integrate over the transverse coordinate, which is thus eliminated by the orthonormality of the basis set. We obtain the expression

$$i\hbar \frac{\partial \phi_m}{\partial t} = -\frac{\hbar^2}{2m} \frac{\partial^2 \phi_m}{\partial s^2} + [V(s,0) + E_n(s)] \phi_m$$

$$+ \sum_{n=0}^{\infty} X_{nm}(s) \frac{\partial^2 \phi_n}{\partial s^2} + A_{nm}(s) \frac{\partial \phi_n}{\partial s} + B_{nm}(s) \phi_n, \tag{12}$$

where we have introduced the off-diagonal mass matrix elements

$$X_{n,m}(s) = \frac{\hbar^2}{m} \int_{-\infty}^{\infty} \eta_n(s,\xi) \kappa(s) \xi \eta_m(s,\xi) d\xi, \tag{13}$$

and the kinetic couplings

$$A_{n,m}(s) = -\frac{\hbar^2}{2m} \int_{-\infty}^{\infty} \eta_n(s,\xi) \left[[2\kappa(s)\xi - 1] \frac{\partial}{\partial s} - \frac{\partial\kappa(s)}{\partial s} \xi \right.$$

$$\left. + 3 \frac{\partial\kappa(s)}{\partial s} \kappa(s) \xi^2 \right] \eta_m(s,\xi) d\xi, \tag{14}$$

and the potential couplings

$$B_{n,m}(s) = \frac{\hbar^2}{2m} \int_{-\infty}^{\infty} \eta_n(s,\xi) \left[[2\kappa(s)\xi - 1] \frac{\partial^2}{\partial s^2} + \frac{\partial\kappa(s)}{\partial s} \right.$$

$$\left. \times [\xi - 3\kappa(s)\xi^2] \frac{\partial}{\partial s} - \kappa(s) \frac{\partial}{\partial \xi} \right] \eta_m(s,\xi) d\xi. \tag{15}$$

The couplings (14) introduce velocity dependent interactions.

III. ADIABATICITY CONDITIONS

If the potential-energy surface changes sufficiently slowly over lengths comparable with the de Broglie wavelengths of the wave packet, we expect that the couplings between transverse states will be negligible. As a consequence, the corresponding one-dimensional equations will decouple resulting in adiabatic following in the transverse states as the wave packet propagates in the longitudinal direction. For most cases, the expansion of a smooth wave packet in the adiabatic eigenbasis $\{\eta_n(s,\chi)\}$ converges rapidly, and allows us to retain only a limited, in many cases small number of transverse levels. As we have already seen, there are two types of changes in the coordinate system that might cause nonadiabatic transitions. First there is curving of the minimal path along the path length. As this is similar to the Coriolis effect in classical mechanics it will cause the wave packet to be displaced in the transverse direction, something that can be induced only by a parity breaking coupling between the levels. This type of nonadiabaticity will, in other words, cause transitions between adjacent levels. Second, there is the change in curvature of the transverse potential which will cause the isopotential lines to converge or diverge along the longitudinal coordinate. This will only cause changes in a symmetric fashion and thus only connect levels with the same parity, i.e., levels separated by at least another level with different parity. Here only nonadiabaticity of the second type, i.e., squeezing, will be treated and displacement is left for further investigations.

In order to derive a condition for adiabaticity, we have to compare the time scales of internal dynamics of the transverse motion with the time scale of change in the transverse potential as the wave packet traverses along the minimal curve. In the spirit of dimensional analysis we make an estimate of the influence of the potential parameters on the adia-

baticity. For a harmonic oscillator the dynamic time scale is given by the oscillator frequency

$$T = \frac{2\pi}{\omega_0}. \tag{16}$$

We consider the longitudinal motion to be that of a classical point particle traveling along the potential minima, the center-of-mass (cm) motion thus described by a given velocity. In a frame moving along with the particle, the transverse dynamics will then be governed by an harmonic oscillator with time-dependent frequency

$$\omega(x_{CM}(t)) = \omega(x_0 - vt). \tag{17}$$

The time derivative of the frequency in the comoving frame will be

$$\frac{\partial \omega(x_{CM}(t))}{\partial t} = \frac{\partial \omega(x_{CM}(t))}{\partial x} \frac{\partial x_{CM}(t)}{\partial t} = \frac{\partial \omega(x_{CM}(t))}{\partial x} v$$

$$\approx \frac{\Delta \omega}{L} v, \tag{18}$$

where the final step was arrived at by taking the derivative of transverse frequency to be the amount of frequency change divided by the appropriate length scale. The time scale over which sizable changes in the oscillator frequency occur is given by

$$\Delta t = \frac{\omega}{\frac{\partial \omega}{\partial t}} = \frac{mL\omega_0 \lambda}{2\pi\hbar\Delta\omega}, \tag{19}$$

where the final equality results from the use of Eq. (18) and expressing the classical velocity in terms of the corresponding de Broglie wavelength. The adiabatic theorem states that transitions between levels will be negligible if the changes in the potential occur over a much longer time scale than that of the internal dynamics. This gives us the condition

$$A \equiv \frac{T}{\Delta t} = \frac{(2\pi)^2 \hbar \Delta \omega}{mL\lambda\omega_0^2} \ll 1. \tag{20}$$

This parameter A is known as the Massey parameter in semiclassical quantum mechanics [17], and is frequently used to indicate whether or not a system will evolve adiabatically under a perturbation. It can be seen from Eq. (20) that, in order to allow adiabatic propagation of wave packets in this potential, changes of the oscillator frequency must occur over sufficiently long time scales and also that larger level separations are preferred, as this makes the transverse time scale shorter thus allowing more rapid changes of the potential.

IV. NUMERICAL TEST OF ADIABATICITY

When the coupling between the levels in the harmonic-oscillator model is weak enough to be neglected, the full problem can be described by the set of equations

$$i\hbar \frac{\partial \phi_n}{\partial t} = -\frac{\hbar^2}{2m} \frac{\partial^2 \phi_n}{\partial^2 s} + A_{nn}(s) \frac{\partial \phi_n}{\partial s}$$

$$+ \left[\hbar \omega(s) \left(n + \frac{1}{2} \right) + B_{nn}(s) \right] \phi_n, \tag{21}$$

where the potential-energy variation along the minimal curve $V(s,0)$ has been chosen to be zero as it will not influence the dynamics under consideration. We obtain an approximation for the total wave function from Eq. (5) using the numerical solution of Eq. (21), and the transverse wave functions from Eq. (10). This is compared with the full numerical solution of Eq. (1), and we test the validity of adiabaticity when the parameter A of Eq. (20) is varied. For a linear potential minimum, all curvature terms disappear and the Laplacian has the familiar Cartesian form. The solution of the coupled problem will be the exact solution. Here we consider propagation in the ground-state mode as this is the case in many situations of interest, such as quantum information applications and interferometric measurements. A natural measure of the difference between two wave functions in this case is the L^2 norm [20,21] of their difference; here we use the square for convenience as this also measures probability in quantum mechanics

$$\varepsilon(t) = ||\Psi_{2D}(s,\xi,t) - \Psi_0(s,\xi,t)||^2$$

$$= \int_{-\infty}^{\infty} \int_{-\infty}^{\infty} |\Psi_{2D}(s,\xi,t) - \phi_0^A(s,t)\eta_0(\xi,s)|^2 d\xi ds, \tag{22}$$

where $\phi_0^A(s,t)$ is the longitudinal wave function obtained from solving Eq. (21) with only one channel, thus corresponding to adiabatic propagation in the transverse ground-state mode. If $\Psi_{2D}(s,\xi,t)$ is calculated using the coupled set of equations in Eq. (12) the expression for $\varepsilon(t)$ simplifies to

$$\varepsilon(t) = \int_{-\infty}^{\infty} |\phi_0(s,t) - \phi_0^A(s,t)|^2 ds + \sum_{n=1}^{\infty} P_n(t), \tag{23}$$

where $P_n(t)$ denotes the total probability of population in the transverse mode n at time t. It is seen that $\varepsilon(t)$, in addition to the probability of being excited to higher transverse modes also measures the redistribution of ground-state probability in the longitudinal direction, due to interaction with the other modes. To test for adiabaticity with respect to changes in the transverse curvature, we choose a potential with a ground-state energy varying along the minimal path as

$$V(s,\xi) = \frac{1}{2} m\omega(s)^2 \xi^2, \tag{24}$$

where the oscillator frequency $\omega(s)$ is taken to be of the form

$$\omega(s) = \omega_0 + \frac{\Delta \omega}{1 + \exp(-s/L)}. \tag{25}$$

For $\Delta\omega > 0$ this potential has an increasing transverse oscillator frequency along the longitudinal coordinate and will resemble a narrowing bottleneck. In this situation the local coordinate frame given by (s,ξ) coincides with the usual Cartesian coordinates (x,y). The coupling matrix elements simplify considerably in this case, and they can be calculated explicitly giving

$$A_{n,m}(s) = \frac{\hbar^2}{8m} \frac{\omega_s(s)}{\omega(s)} (\sqrt{(m+1)(m+2)}\,\delta_{n,m+2} - \sqrt{m(m-1)}\,\delta_{n,m-2}),$$

(26)

and

$$B_{n,m}(s) = -\frac{\hbar^2}{8m}\left\{ \left(\frac{\omega_s(s)}{\omega(s)}\right)^2 (\sqrt{(m+1)(m+2)(m+3)(m+4)}\,\delta_{n,m+4} - 2(m^2+m+1)\delta_{n,m} \right.$$

$$\left. + \sqrt{m(m-1)(m-2)(m-3)}\,\delta_{n,m-4}) + \left[\frac{\omega_{ss}(s)}{\omega(s)} + \left(\frac{\omega_s(s)}{\omega(s)}\right)^2\right](\sqrt{(m+1)(m+2)}\,\delta_{n,m+2} - \sqrt{m(m-1)}\,\delta_{n,m-2}) \right\},$$

(27)

where

$$\omega_s(s) = \frac{\partial\omega(s)}{\partial s}, \quad \omega_{ss}(s) = \frac{\partial^2\omega(s)}{\partial s^2},$$

(28)

are the derivatives of the oscillator frequency taken with respect to the longitudinal coordinate. Because the potential in Eq. (24) resembles a bottleneck, the wave packet has to squeeze itself into a more tightly confined region when propagating. Depending on whether or not the change in oscillator frequency is slow enough at the kinetic energy under consideration, the wave packet may either penetrate smoothly into the narrow region, or be reflected to a degree depending on its kinetic energy. In general it acquires transverse breathing due to nonadiabatic transitions.

The Eqs. (1) [or equivalently Eq. (12)] and (21) have no known analytical solution for the potential under consideration, so we have to resort to numerical methods for further studies. For clarity all equations have been given in dimensional form up to this point. In the numerical work presented further on, dimensionless units are used for convenience.

The choice of dimensionless unities for mass, time, and oscillator frequency together with the special choice for the two physical constants is equivalent to introducing a special rescaling. The dimensionful variables of length and time and also of the oscillator frequency are rescaled according to

$$s \to \frac{s}{S},$$

$$\xi \to \frac{\xi}{X},$$

$$t \to \frac{t}{T},$$

$$\omega \to \frac{\omega}{\Omega}.$$

(29)

This scaling introduced into Eq. (4) together with Eq. (24) for the transverse binding potential gives us in the new rescaled variables

$$i\frac{\partial\Psi}{\partial t} = \frac{\hbar T}{mS^2}\left(-\frac{1}{2}\frac{\partial^2\Psi}{\partial s^2}\right) + \frac{\hbar T}{mX^2}\left(-\frac{1}{2}\frac{\partial^2\Psi}{\partial\xi^2}\right)$$

$$+ \left(\frac{mTX^2}{\hbar}\right)\frac{1}{2}\omega(s)^2\xi^2\Psi.$$

(30)

The terms dependent on the curvature are omitted here. All the prefactors multiplying each term on the right-hand side of Eq. (30) now have to be set to unity to comply with our choice of dimensionless units. From the resulting equations we get the following relations among the scale parameters:

$$S = X = \sqrt{\frac{\hbar\Omega}{m}},$$

$$T = \frac{1}{\Omega}.$$

(31)

There is thus only one scale parameter that can be chosen arbitrarily, the other will follow. From the form of Eqs. (31) we see that requiring the three dimensionless prefactors in Eq. (30) to equal unity is consistent with choosing this one physical scale parameter (length, time, or oscillator frequency) and letting the other two (since the two length scales are equal) be the characteristic values for a harmonic oscillator which is determined by the first parameter choice. It should be noted that this choice of harmonic oscillator does not have to coincide with the actual one given by the transverse binding potential. It only serves as a reference for the scaling procedure whereas the physical binding potential will be given in terms of this reference for the numerical simulations.

A numerical example of wave-packet propagation is illustrated in Figs. 1–4, where a potential of the bottleneck type described in Eqs. (24) and (25) has been used with the di-
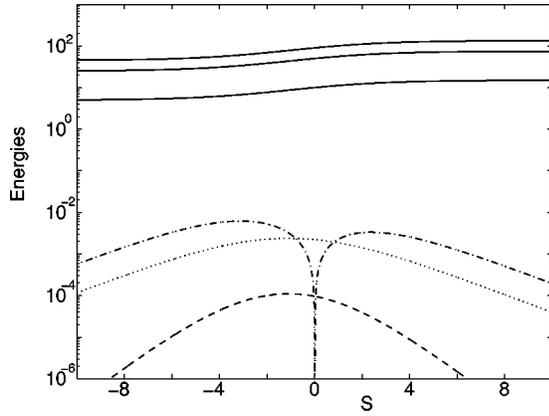
FIG. 1. The three lowest adiabatic energies in dimensionless units, i.e., $E_n(s) + B_{nn}(s)$ for $n = 0$, 2, and 4 (solid lines), together with the couplings between the ground state and the other two levels as functions of the longitudinal distance, also in dimensionless units. Shown here are dotted $A_{20}(s)$, dash dotted $|B_{20}(s)|$, and dashed $|B_{40}(s)|$. It is seen that the potential coupling $B_{20}(s)$ has a zero for $s = 0$, where the transverse oscillator frequency has an inflection point.

mensionless parameter values $\omega_0 = 10$, $\Delta\omega = 20$, and $L = 2$. In addition the longitudinal momentum has been chosen to be $k = 40$.

The diagonal potential couplings together with the transverse eigenenergies, i.e., $E_n(s) + B_{nn}(s)$, act as effective one-dimensional potentials in the adiabatic limit, and they are here referred to as adiabatic energies. For the bottleneck potential they experience an increase with longitudinal distance as is shown by solid lines in Fig. 1 for the modes $n = 0$, 2, and 4. This increase is directly proportional to the mode number for harmonic transverse potentials, thus affecting the higher modes more with the higher mode number. The nonadiabatic dynamics is determined by the strength of the couplings, given by Eqs. (13)–(15) which also show an
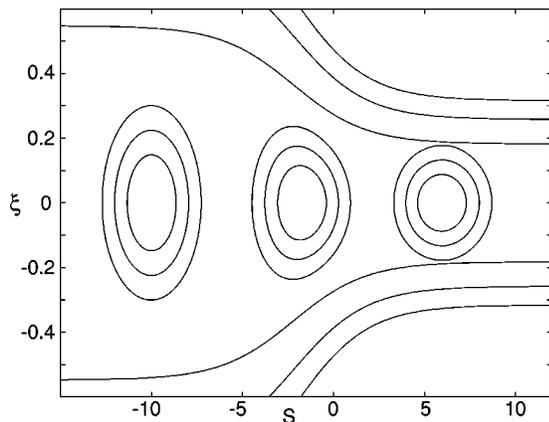

FIG. 2. Snapshots taken at the times $t = 0$, $t = 0.2$, and $t = 0.4$ of a Gaussian wave packet with longitudinal width $\Delta s = 8$ propagating through the bottleneck potential given by Eq. (24). The wave packet adjusts itself in the transverse direction as it progresses through the bottleneck, and no signs of nonadiabaticity can be seen. Both coordinates are in the dimensionless units used in the numerical work as explained in Sec. IV.
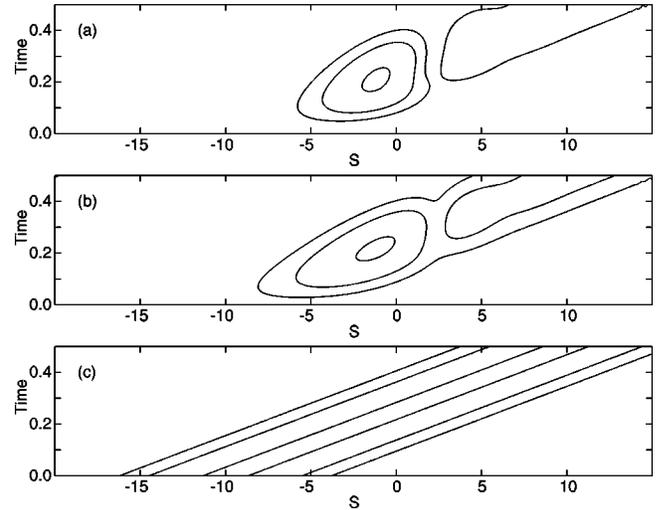

FIG. 3. Contour plots of the probability density, $|\phi_n(s,t)|^2$ for the three lowest even longitudinal wave functions. The contour levels give the probability density at 80%, 8%, and 0.8% of the peak value in each mode. The ground-state mode, shown in (c), is seen to propagate through the bottleneck with negligible retardation and no visible depletion due to excitation. The first even excited state, $n = 2$, shown in (b), starts to be populated as the wave packet for the ground state mode approaches the region around $s = 0$ where the couplings peak, as can be seen in Fig. 1. The population peaks as the wave packet in the ground-state mode passes $s = 0$, and diminishes after that, and we are left with a remnant population due to nonadiabatic transitions as the wave packet leaves the interaction region. For the highest mode $n = 4$, shown in (a), the spatiotemporal evolution is similar as the one for $n = 2$, albeit at a smaller value of the probability density; see Fig. 4. Both the time axis and longitudinal coordinate are in the dimensionless units used here.

increasing strength for higher modes. In Fig. 1 the potential and kinetic couplings between the ground state and $n = 2$ and $n = 4$, are shown as functions of the longitudinal distance. It is seen that whereas the kinetic coupling $A_{20}(s)$, shown dotted, and the potential coupling $B_{40}(s)$, shown dashed, go through a maximum and decrease away from the center of the bottleneck, the potential coupling $B_{20}(s)$, shown dash dotted, has a zero at the inflection point $s = 0$.

A wave packet propagating through the potential structure given by Eqs. (24) and (25) will have to squeeze itself in through the bottleneck, if the kinetic energy is sufficient, and adjust its width to the more tightly confining transverse oscillator frequency. This is seen in Fig. 2 where the probability density for a Gaussian wave packet of length $\Delta s = 8$ is shown at three consecutive times while propagating in a potential with the dimensionless parameters given above.

The dynamics of the longitudinal wave functions can be seen in Fig. 3 that shows contour plots of the probability density $|\phi_n(s,t)|^2$ of the three lowest even longitudinal wave functions. The ground-state mode is seen to propagate through the bottleneck with negligible retardation and no visible depletion due to excitation into higher modes. The first even excited state starts to be populated as the wave packet for the ground-state mode approaches the region around the inflection point where the couplings peak, as can be seen in
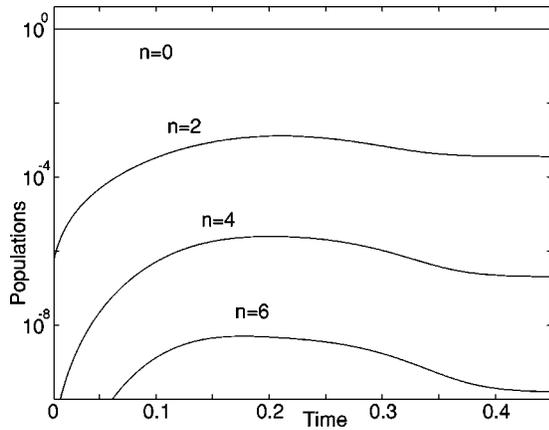
FIG. 4. Total level populations for the four lowest even transverse modes versus propagation time. The temporal behavior of the level populations reflects the spatial structure of the couplings and the fact that the wave packet is spatially localized along the longitudinal coordinate. As the bulk of probability density, which resides in the ground-state mode, propagates through the bottleneck, as is seen in Figs. 2 and 3, the populations in the higher modes increase until the inflection point at $s=0$ is reached around $t \approx 0.2$, and starts to decrease after that. Beyond the passage of the inflection point, the populations decrease until most of the wave packet has propagated out of the interaction region around the bottleneck, and then settle at their asymptotic values as no more transitions can take place. The time axis is in dimensionless units.

Fig. 1. The population peaks as the wave packet in the ground-state mode passes the region around $s=0$, and diminishes after that, and we are left with a remnant population due to nonadiabatic transitions as the wave packet leaves the interaction region. For the highest mode shown here, $n=4$, the spatiotemporal evolution is similar to that for $n=2$, albeit at a smaller value of the probability density.

The temporal behavior of the total level populations, see Fig. 4, reflects the spatial structure of the couplings together with the fact that the wave packet is spatially localized over a finite region along the longitudinal coordinate and interacts most strongly over only a limited longitudinal interval. The bulk of probability density resides in the ground-state mode, and when this mode propagates through the bottleneck, as is seen in Figs. 2 and 3, the populations of the higher modes increase until the inflection point is reached around $t \approx 0.2$, and then start to decrease. After passing the inflection point, the populations decrease until most of the wave packet has propagated out of the interaction region around the bottleneck, and then saturate at their asymptotic values when no further transitions can take place.

As the potential is given by Eq. (24) together with Eq. (25), the problem contains no less than four parameters: ingoing oscillator frequency ω_0, change in oscillator frequency $\Delta \omega$, length scale L for change of the transverse frequency, and the initial longitudinal momentum k. A random scan has been performed where the four dimensionless parameters were varied over an accessible region of the parameter space in such a way that the points were equidistributed on a logarithmic scale for each parameter. All four quantities $(\omega_0, \Delta \omega, L, k)$ were varied over at least two orders of mag-
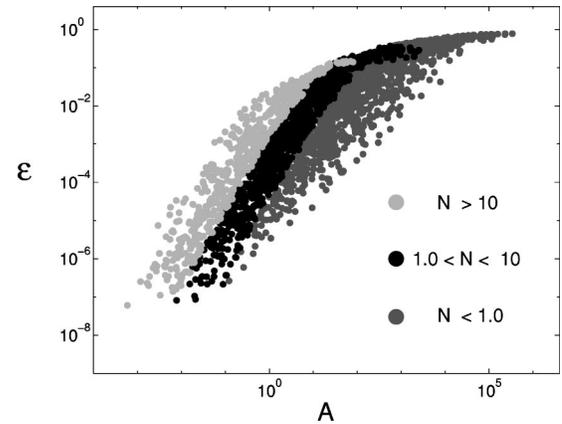

FIG. 5. Scatter plot of the total excited population ε versus the Massey parameter A as given by Eq. (20). The data has been shaded according to three intervals for the Fresnel parameter N as defined in Eq. (37). It is clearly seen that although the spread in ε is large when plotted versus the adiabaticity parameter, we still can tell whether or not there will be adiabatic propagation simply by calculating the Fresnel number and checking whether or not this is small.

nitude in a region considered to be of physical interest in applications of wave-packet methods. The intervals of variation for the parameters were

$$10^{-1} \leqslant \omega_0 \leqslant 10, \tag{32}$$

$$10^{-3} \leqslant \Delta \omega \leqslant 10, \tag{33}$$

$$10^{-1} \leqslant L \leqslant 10, \tag{34}$$

$$10 \leqslant k \leqslant 160. \tag{35}$$

In order to explore the phenomenology of this simple propagation model, 6000 parameter combinations were chosen randomly in the parameter space delimited by Eqs. (32)–(35), and a wave packet was propagated numerically through the bottleneck potential using a pseudospectral method [22,23] for both a 2D wave packet and an adiabatic wave packet in the ground state. The resulting deviation in norm between the two wave packets was calculated using Eq. (22). A scatter plot of the resulting norm difference versus adiabaticity parameter A, is shown in Fig. 5 where it can be seen that $A \approx 0.8$ an upper limit below which the wave packet within a probability of more than 0.99, stays in the ground-state mode. It is also seen that even if the majority of the cases considered here behave largely as expected from our simplified analysis of adiabaticity in Sec. III, there is, however, a large number of cases having excitations far below what would be expected from using the Massey parameter alone.

V. INTERPRETATIONS

The parameter scans have to be analyzed in order to find any possible regularities that might indicate how adiabaticity will manifest itself in our simple model system. Our first attempt was to plot in Fig. 5 the norm difference versus the adiabaticity parameter defined as A in Eq. (20). This in itself
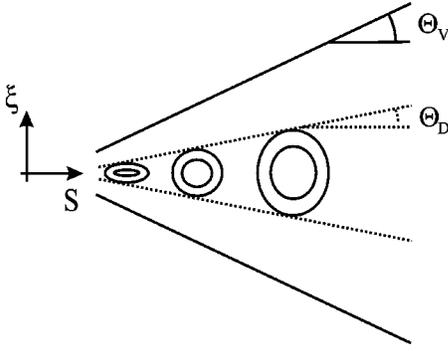
FIG. 6. Schematic picture showing the definition of the angles used in the derivation of the diffraction criterium. The diffraction angle Θ_D is defined by the opening angle for a hypothetical cone, here shown dashed, swept out by the equiprobability lines of a wave packet propagating through the potential whereas the potential opening angle Θ_V is shown solid. This is defined by the solid equipotential lines. Units on both axes are taken to be dimensionless.

does, however, not show more than a general trend as the results cover a substantial region of the parameter space. Thus for a given value of the Massey parameter A, the spread is too large to allow us to conclude whether or not we will be in the adiabatic regime by using only this single parameter as a measure. An investigation in terms of other dimensionless parameters reveals that there exists additional structure in the dataset. For a given value of the relative change in oscillator energy $\Delta\omega/\omega_0$, we wish to determine what maximum wave-packet momenta can be used and over which length scales the potential may change in order to avoid nonadiabatic transitions into higher transverse states.

It is reasonable to assume that the free spreading of the wave packet ultimately will be limiting the change of the potential in the transverse direction and still allows adiabatic propagation. The free spreading is governed by the transverse momentum distribution, which in turn is related to the initial width of the potential. The situation is very similar to beam diffraction in optics and laser theory [24], where field distributions evolve into fully opened beams over distances larger than or comparable with the Rayleigh length

$$z_R = \frac{a^2}{\lambda}, \qquad (36)$$

where a is the width of the aperture. The number of Fresnel zones contributing to the diffraction pattern at a distance z is given by the Fresnel number, which for a square aperture is given by the expression

$$N = \frac{z_R}{z} = \frac{a^2}{z\lambda}. \qquad (37)$$

Small Fresnel numbers correspond to the far-field zone where the transverse distribution is determined by the contribution from a single Fresnel zone only.

In the case of matter waves the diffraction situation may be illustrated in Fig. 6 for a wave packet propagating through a potential that is changing in the transverse direction. The

equipotential lines, shown solid in Fig. 6, diverge at an angle Θ_V for which we have, using the length L and the initial and final oscillator widths, the expression

$$\tan(\Theta_V) = \frac{1}{L}\left(\frac{1}{\sqrt{\omega_0}} - \frac{1}{\sqrt{\omega_0 + \Delta\omega}}\right)$$

$$= \frac{1}{\sqrt{\omega_0}L}\left(1 - \frac{1}{\sqrt{1 + \dfrac{\Delta\omega}{\omega_0}}}\right). \qquad (38)$$

For a wave packet propagating in a widening potential, the equiprobability lines traced out during the evolution will diverge and given that the widening is not too rapid, adjustment to the new width will take place. An upper limit for how fast this spreading can be, is set by the free spreading, which will occur at a rate corresponding to an angle Θ_D shown in Fig. 6. This is taken to be equivalent to the diffraction angle of a free Gaussian beam of width $\Delta\xi$, given by

$$\tan\Theta_D = \frac{\Delta k_T}{k} = \frac{1}{k\Delta\xi} = \frac{\sqrt{\omega_0}}{k} = \frac{\lambda}{2\pi}\sqrt{\omega_0}, \qquad (39)$$

where the widths of the transverse distributions in momentum and coordinate space are related by

$$\Delta\xi\Delta k_T = 1, \qquad (40)$$

since the transverse probability distribution will be a minimal uncertainty state given that the evolution is adiabatic. Using Eqs. (38) and (39) and requiring that the beam diffraction angle should be larger than the potential changing angle, which is a minimal requirement for adiabatic following, we have

$$\frac{\tan\Theta_V}{\tan\Theta_D} = \frac{2\pi}{L\lambda\omega_0}\left(1 - \frac{1}{\sqrt{1 + \dfrac{\Delta\omega}{\omega_0}}}\right) \equiv Ng\left(\frac{\Delta\omega}{\omega_0}\right) < 1, \qquad (41)$$

where the Fresnel number for this situation is given in dimensionally correct units as

$$N = \frac{\hbar}{mL\lambda\omega_0}. \qquad (42)$$

In order to relate this to the case of potential narrowing, we consider the time-reversal symmetry of quantum mechanics. In the current situation this implies that a wave packet moving to the left in Fig. 6 must obey the same adiabaticity conditions as one moving to the right as the time reversal is equivalent to momentum reversal for the plane-wave components of the wave packet. It is thus seen that the transverse evolution of a wave packet is limited by diffraction no matter if the change is to a wider or a narrower potential.

We see from Eq. (41) that the ratio is given by the product of the Fresnel number and a function of the relative change of the oscillator width. The function $g(\Delta\omega/\omega_0)$ varies be-

tween zero (for $\Delta\omega/\omega_0 = 0$) and 2π, which is rapidly approached for large arguments. For small changes of the transverse momentum, the function $g(\Delta\omega/\omega_0)$ can be Taylor expanded, giving an additional factor of $\Delta\omega/\omega_0$ making the ratio in Eq. (41) identical with the Massey parameter as defined by Eq. (20). In Fig. 5 the data from our random scan has been divided into three sets with respect to the values of the Fresnel parameter N, which clearly orders the different combinations in a systematic way. Is is seen that adiabaticity can be achieved even when the Massey parameter is larger than unity, provided that the Fresnel parameter is small enough. It appears that it is not primarily a local criterium given by Eq. (20) which decides if adiabatic propagation will take place, but rather whether or not the changes are such that the Fresnel parameter is small. Thus it is more the question of whether or not the changes occur over a length scale comparable to or larger than the Rayleigh length. This is the length a free beam requires in order to redistribute its transverse momentum components into its new angular distribution; this is set by diffraction. The numerical searches, as described in the previous sections, have shown that adiabaticity in this system is governed by the value of the Fresnel parameter given by Eq. (42).

To investigate our findings, a limited region of parameter space has been chosen for a structured scan with higher resolution in order to explore the transition region where adiabatic behavior begins to dominate. An ordered and systematic scan involving all four parameters would be too time consuming and also difficult to analyze, consequently the longitudinal momentum and transverse oscillator frequency were set to fixed values whereas the increase of the transverse frequency and the corresponding length scale were varied, which brings the scan down to two dimensions. This should not be considered a limitation since it has been seen in the random scan that the phenomenology is captured by two dimensionless parameters. The values were chosen to be

$$\omega_0 = 5, \tag{43}$$

$$0 \leq \Delta\omega \leq 20, \tag{44}$$

$$5 \times 10^{-2} \leq L \leq 5, \tag{45}$$

$$k = 70. \tag{46}$$

The results of this scan are shown in Fig. 7, a contour plot for the deviation parameter ε as function of Fresnel parameter N and frequency squeeze $\Delta\omega/\omega_0$ for the region in question. For large values of the Fresnel parameter, the equideviation lines become straight lines implying independence of this parameter. The deviation is in this case a function of only the frequency squeeze, indicating that large values of the Fresnel parameter corresponds to the sudden limit as the deviation only depends on the amount of squeezing and no longer on the rate at which it is done. For smaller values of the Fresnel parameter, especially below unity, the deviation rapidly decreases and the equideviation lines bend towards allowing higher values of frequency squeeze. We see that for low values of the Fresnel parameter, it will be possible to
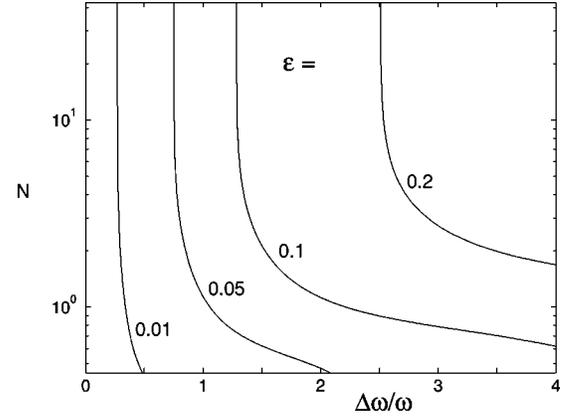

FIG. 7. Contour levels of ε, the difference in norm versus change in Fresnel parameter N and frequency squeeze $\Delta\omega/\omega_0$. Here it can clearly be seen that the excitation, which has been taken as measure for deviation from adiabaticity, has a strong dependence on the Fresnel parameter. It appears that very large frequency squeezes can be achieved only if the Fresnel parameter is kept small, which does not necessarily imply that the Massey parameter is small. Both axes are dimensionless.

perform substantial frequency squeezes and still retain almost all of the population in the lowest transverse mode, thus achieving adiabatic propagation in the potential under consideration.

As indicated by the vertical equideviation lines in Fig. 7 we can reach the limit opposite to the adiabatic, viz. the sudden approximation, for large values of the Fresnel parameter when the transverse states change rapidly. In this case the wave packet may be considered to have propagated into the narrow region without any readjustment of its shape. Then the wave packet will behave in the transverse direction like a squeezed state, and the expansion into the different modes can be carried out [25] simply by projecting the incoming Gaussian ground state onto the outgoing, more tightly confined, oscillator states. An estimate for the excitation is then given by subtracting the absolute value squared of the projection

$$\varepsilon_{sudden} \equiv \| \eta(\omega_0) - \eta(\omega_0 + \Delta\omega) \|^2 = \langle [\eta_0(\omega_0) - \eta(\omega_0$$
$$+ \Delta\omega)] | [\eta_0(\omega_0) - \eta(\omega_0 + \Delta\omega)] \rangle$$
$$= 2[1 - \langle \eta_0(\omega_0) | \eta_0(\omega_0 + \Delta\omega) \rangle]$$
$$= 2 \left[1 - \left(\frac{\sqrt{1 + \Delta\omega/\omega_0}}{1 + \frac{1}{2}\Delta\omega/\omega_0} \right)^{1/2} \right]. \tag{47}$$

For large values of the Fresnel parameter, this should give a reasonable approximation to the deviation from adiabatic following in the ground-state mode.

From the data in Fig. 5 we choose the ones with Fresnel parameter $N > 10$, and in Fig. 8 we show the deviation versus frequency squeeze, $\Delta\omega/\omega_0$ together with the analytical estimate given by Eq. (47) for comparison. It is seen that the simple estimate by Eq. (47) is reasonable over most of the interval. It is not clear to us to what extent the small discrep-
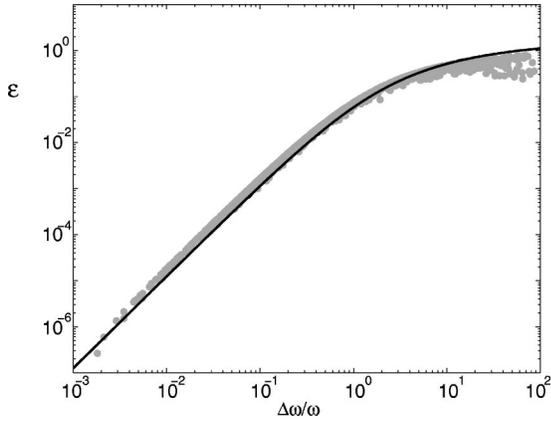
FIG. 8. A scatter plot of the norm difference versus squeeze parameter $\Delta\omega/\omega_0$ for parameter combinations with Fresnel parameter $N > 10$. Also shown is the analytic estimate using the projection between ingoing and outgoing transverse ground states to calculate the norm difference as given by Eq. (47). The agreement can be seen to be reasonable although a systematic deviation resulting in an underestimate of about 10–20 % with respect to Eq. (47) is present for smaller frequency squeezes. Both axes are dimensionless.

ancy seen in Fig. 8 is due to numerical inaccuracies in the wave-packet calculations, especially deriving from the finiteness of the spatial simulation region.

VI. CONCLUSIONS

We have explored the propagation of longitudinal wave packets in a potential with spatially changing transverse oscillator frequency for various parameter combinations covering a large region of the physically relevant parameter space. We can conclude that the adiabaticity or Massey parameter alone does not decide whether or not adiabatic propagation will take place. Instead of one parameter two are seen to be necessary, the relative change in oscillator energy and the Fresnel parameter $N = \hbar/mL\lambda\omega_0$. Using these two parameters adiabaticity can be achieved even for cases when the Massey parameter A takes on values much greater than unity. The criteria given by Eq. (20) has earlier been shown to be connected to the fastest changes allowed by diffraction [26]. We have here shown that the maximal angle, as allowed by diffraction can be reached in different ways and that the evolution will be adiabatic only in the cases when the transition occurs over a length scale comparable with or larger than the Rayleigh length, which corresponds to the Fresnel parameter as given by Eq. (42) being smaller than unity.

The consequences for different applications can be estimated with straightforward estimates. For electrons in semiconductors, for instance, in a quantum wire configuration, coherent phenomena are limited to time scales set by scattering events, which for GaAs in bulk samples results in coherence times on the order of $\tau_\phi \approx 200$ fs. Assuming that this limits the length scales over which adiabatic propagation will occur we have

$$L \approx v\,\tau_\phi = \frac{2\pi\hbar}{m\lambda}\,\tau_\phi. \tag{48}$$

Inserting this into our expression for the Fresnel parameter and requiring this to be smaller than one gives us

$$N = \frac{\hbar}{mL\lambda\omega_0} = \frac{1}{2\pi\omega_0\tau_\phi} \lesssim 1. \tag{49}$$

This result is determined by the diffraction condition here, combined with the time interval set by incoherent phenomena. Then the condition that the wave packet propagates adiabatically simplifies to the condition that at least one internal oscillation time should have passed within this time interval. Expressing the Fresnel parameter in terms of the ground-state width, here denoted by $\Delta\xi$, we have

$$N = \frac{\hbar}{mL\lambda\omega_0} = \frac{\Delta\xi^2}{L\lambda}. \tag{50}$$

Inserting the expression above for the length L, we find for the ground-state width the expression

$$\Delta\xi \lesssim \sqrt{\frac{\hbar 2\pi\tau_\phi}{m}}. \tag{51}$$

Assuming, as for instance in GaAs, an effective mass of 0.07 electron masses, results in an upper limit of $\Delta\xi \lesssim 100$ nm, roughly consistent with present day experimental conditions if the longitudinal extent is at least of the order of the coherence length. For quantum point contacts, this might not be the case, and adiabaticity will have to be decided by numerical simulations for the relevant conditions.

For atom optics in effectively one-dimensional geometries, the width of the ground state is roughly tenths of microns and the de Broglie wave length around or below 1 μm for temperatures in magneto-optically trapped Rubidium. This gives us, using Eq. (50), a Fresnel parameter below unity for length scales around at least tens of nanometers, clearly not a restriction for present day experiments.

In optical waveguide theory, the main interest lies in the situations where only a single mode will contribute to the propagation, although optoelectronic components with tapered guides may enter the region of multimode propagation. For a single-mode fiber, nonadiabaticity inevitably leads to losses due to coupling with continuum states lying above the confining barrier provided by the refractive indices of cladding and core [18]. Criteria for achieving adiabatic, i.e., lossless, propagation have been derived [27] and have been found to be related to classical diffraction effects. These results are consistent with those given here although the electromagnetic propagation equations are different.

We have found that a condition for adiabaticity in atom optics is determined by diffraction rather than from the Massey parameter that is based on semiclassical considerations. This suggests two conclusions: Firstly it may be concluded that quantum mechanics appears to be more robust with respect to nonadiabatic perturbations than one may expect using arguments from classical mechanics. Secondly, the re-

sults indicate that there is a fundamental relation between diffraction and adiabaticity in quantum mechanics, something that derives from the fact that the wave nature is important in quantum dynamics whereas this aspect is absent in the classical mechanics of particles. The adiabatic approximation is thus seen to provide further insights into the fundamentals of quantum mechanics, just as it did in the early developments of the theory.

[1] H.J. Metcalf and P. van der Straten, *Laser Cooling and Trapping* (Springer, New York, 1999).

[2] C.S. Adams, M. Sigel, and J. Mlynek, Phys. Rep. **240**, 143 (1994); J.P. Dowling, and J. Gea-Banaloche, Adv. At., Mol., Opt. Phys. **37**, 1 (1996); E.A. Hinds, and I.G. Hughes, J. Phys. D **32**, R119 (1999).

[3] M. Key, I.G. Hughes, W. Rooijakkers, B.E. Sauer, E.A. Hinds, D.J. Richardson, and P.G. Kazansky, Phys. Rev. Lett. **84**, 1371 (2000).

[4] J. Reichel, W. Hänsel, and T.W. Hänsch, Phys. Rev. Lett. **83**, 3398 (1999); D. Müller, D.Z. Anderson, R.J. Grow, P.D.D. Schwindt, and E.A. Cornell, *ibid.* **83**, 5194 (1999); N.H. Dekker, C.S. Lee, V. Lorent, J.H. Thywissen, S.P. Smith, M. Drndic, R.M. Westervelt, and M. Prentiss, *ibid.* **84**, 1124 (2000); R. Folman, P. Kruger, D. Cassettari, B. Hessmo, T. Maier, and J. Schmiedmayer, *ibid.* **84**, 4749 (2000).

[5] M.J. Renn, D. Montgomery, O. Vdovin, D.Z. Anderson, C.E. Wieman, and E.A. Cornell, Phys. Rev. Lett. **75**, 3253 (1995); H. Ito, T. Nakata, K. Sakaki, M. Ohtsu, K.I. Lee, and W. Jhe, *ibid.* **76**, 4500 (1996).

[6] P. Ehrenfest, Ann. Phys. (Berlin) **51**, 327 (1916).

[7] M. Born, Z. Phys. **40**, 167 (1926).

[8] V. Fock, Z. Phys. **49**, 323 (1928); M. Born and V. Fock, *ibid.* **51**, 165 (1928).

[9] *Quantum Dynamics of Simple Systems*, edited by G.-L. Oppo, S.M. Barnett, E. Riis, and M. Wilkinson (SUSSP Publications, Edinburgh/IOP, London, 1996).

[10] J.H. Thywissen, R.M. Westervelt, and M. Prentiss, Phys. Rev. Lett. **83**, 3762 (1999).

[11] E. Andersson, M.T. Fontenelle, and S. Stenholm, Phys. Rev. A **59**, 3841 (1999).

[12] *Dynamics of Molecules and Chemical Reactions*, edited by J.Z. H. Zhang and R.E. Wyatt (Dekker, New York, 1996); N. Balakrishnan, C. Kalyanaraman, and N. Sathyamurthy, Phys. Rep. **280**, 80 (1997); B.M. Garraway and K.A. Suominen, Rep. Prog. Phys. **58**, 365 (1995).

[13] R.A. Marcus, J. Chem. Phys. **45**, 4493 (1966).

[14] S.-F. Wu and R.D. Levine, Mol. Phys. **22**, 881 (1971).

[15] G.L. Hofacker and R.D. Levine, Chem. Phys. Lett. **9**, 617 (1971).

[16] R.D. Levine, and R.B. Bernstein, *Molecular Reaction Dynamics and Chemical Reactivity* (Oxford University Press, Oxford, 1987).

[17] M.S. Child, *Molecular Collision Theory* (Dover, New York, 1996).

[18] A.W. Snyder and J.D. Love, *Optical Waveguide Theory* (Chapman and Hall, London, 1983).

[19] T. Dittrich, P. Hänggi, G.-L. Ingold, B. Kramer, G. Schön, and W. Zwerger, *Quantum Transport and Dissipation* (Wiley-VCH, Weinheim, 1998).

[20] J.C. Strikwerda, *Finite Difference Schemes and Partial Differential Equations* (Chapman and Hall, New York, 1989).

[21] F. Riesz and B. Sz.-Nagy, *Functional Analysis* (Dover, New York, 1990).

[22] B. Forngren, *A Practical Introduction to Pseudospectral Methods* (Cambridge University Press, Cambridge, England, 1998).

[23] H. Tal-Ezer and R. Kosloff, J. Chem. Phys. **81**, 3967 (1984).

[24] A. Siegman, *Lasers* (University Science Book, Sausolito, California, 1986).

[25] C. Aslangul, Am. J. Phys. **63**, 1921 (1995).

[26] A. Yacoby and Y. Imry, Europhys. Lett. **11**, 663 (1990).

[27] J.D. Love, W.M. Henry, W.J. Stewart, R.J. Black, S. Lacroix, and F. Gonthier, IEE Proc.-J: Optoelectron. **138**, 355 (1991); J.D. Love, Electron. Lett. **23**, 993 (1987).